Lattice-gas Monte Carlo study of adsorption in pores

Raluca A. Trasca,[1] M. Mercedes Calbi,[1] Milton W. Cole,[1] and Jose L. Riccardo[2]
[1]*Department of Physics, Pennsylvania State University, University Park, Pennsylvania 16802, USA*
[2]*Departamento de Fisica, Universidad Nacional de San Luis, 5700 San Luis, Argentina*
(Received 30 July 2003; published 30 January 2004)

A lattice-gas model of adsorption inside cylindrical pores is evaluated with Monte Carlo simulations. The model incorporates two kinds of sites: (a line of) ''axial'' sites and surrounding ''cylindrical shell'' sites, in the ratio 1:7. The adsorption isotherms are calculated in either the grand canonical or canonical ensembles. At low temperature, there occur quasitransitions that would be genuine thermodynamic transitions in mean-field theory. Comparisons between the Monte Carlo and mean-field theory results for the heat capacity and adsorption isotherms are provided.

DOI: 10.1103/PhysRevE.69.011605 PACS number(s): 68.43.−h, 68.90.+g

I. INTRODUCTION

One of the most exciting fields in condensed matter physics is the study of gases inside porous media [1,2]. Its importance stems from questions of fundamental physics (e.g., dimensional crossover and the role of disorder) and a number of relevant technologies (e.g., catalysis, gas separation, and storage) that utilize porosity. In some systems, the pores are fully interconnected so that a gas atom entering at one point will eventually diffuse throughout the porous domain. In other cases of interest, individual pores are distinct, so that the problem can be thought of as essentially independent pores, with perhaps weak interpore interactions. Many model calculations of this adsorption have been presented. A large fraction of these consider the adsorption domain to consist of independent pores, either for simplicity or because that represents an accurate description of the geometry.

In a recent paper (denoted I), we posited a particularly simple model of a nanoporous environment [3]. That is a lattice-gas model with two kinds of sites. One was a one-dimensional (1D) line of sites, which we call ''axial'' sites. Surrounding each axial site is a set of seven ''cylindrical shell'' sites. The number seven is chosen as an estimate of the ratio of shell to axial densities for atoms of diameter ~ 3.5 Å in a carbon nanotube of radius 7 Å. A cross-section view of the nanotube and the adsorption sites is presented in Fig. 1. Each shell site has four (two laterally, one above, and one below) shell neighbors and one axial neighbor. In the model, there are four interaction energies. V_a is the potential energy of an axial atom due to its interaction with the host material, V_s is that of a shell atom, $-\epsilon$ is the interaction energy between adjacent occupied sites of the same type, where $\epsilon > 0$; ϵ_{sa} is the interaction between axial and shell sites, which could have either sign. Thus, the Hamiltonian is

$$H = N_a V_a + N_s V_s + H_{int}. \tag{1}$$

Here $N_a(N_s)$ is the number of occupied axial (shell) sites and the term H_{int} involves both nearest-neighbor interactions of the same species (axial-axial and shell-shell) and the axial-shell interactions, with their respective couplings.

In I, the adsorption isotherms were evaluated with mean-field theory (MFT). That is, the number of adsorbed particles (henceforth called atoms) was computed for specified reduced temperature $T^* = k_B T/\epsilon$ as a function of the reduced chemical potential $\mu^* = \mu/\epsilon$. The resulting behavior found in I includes a set of transitions associated with filling the respective sites. If $V_a \ll V_s$, the axial sites are occupied first (as μ increases), while the reverse is the case if $V_a \gg V_s$. If, instead, the energies are similar, there arises a ''cooperative transition,'' in which both sites are filled simultaneously at low T and sufficiently high μ. These transitions, however, are artifacts because true thermodynamic transitions cannot exist in 1D. Nevertheless, the behavior in the Monte Carlo solution is here found to be very similar to that of MFT, in that the coverage rises very rapidly near a threshold value of μ. We note, however, that if there exists a transverse coupling between sites in neighboring pores such a genuine transition does occur (at a relatively high T—usually much higher than might be expected from the strength of the interpore interaction) [3–8].

In this paper, we consider the same lattice-gas model as that treated in I. The difference is that we here evaluate the system's properties with the Monte Carlo (MC) simulation technique. MC simulations of the lattice-gas models have been employed in studying a variety of adsorption and diffusion problems [1,2,8–10]. Our method is discussed in Sec. II along with a test of its sensitivity to the assumption of periodic boundary conditions. Section III presents our results and Sec. IV summarizes and comments upon them.

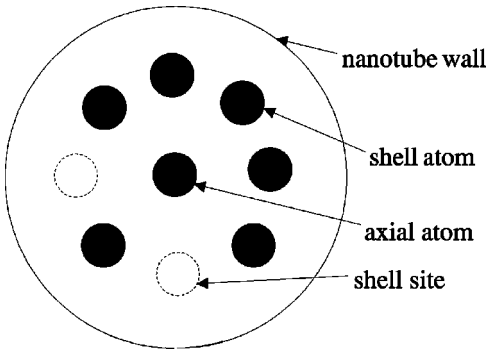

FIG. 1. Schematic transverse section of a nanotube, showing occupied and unoccupied axial and shell sites.

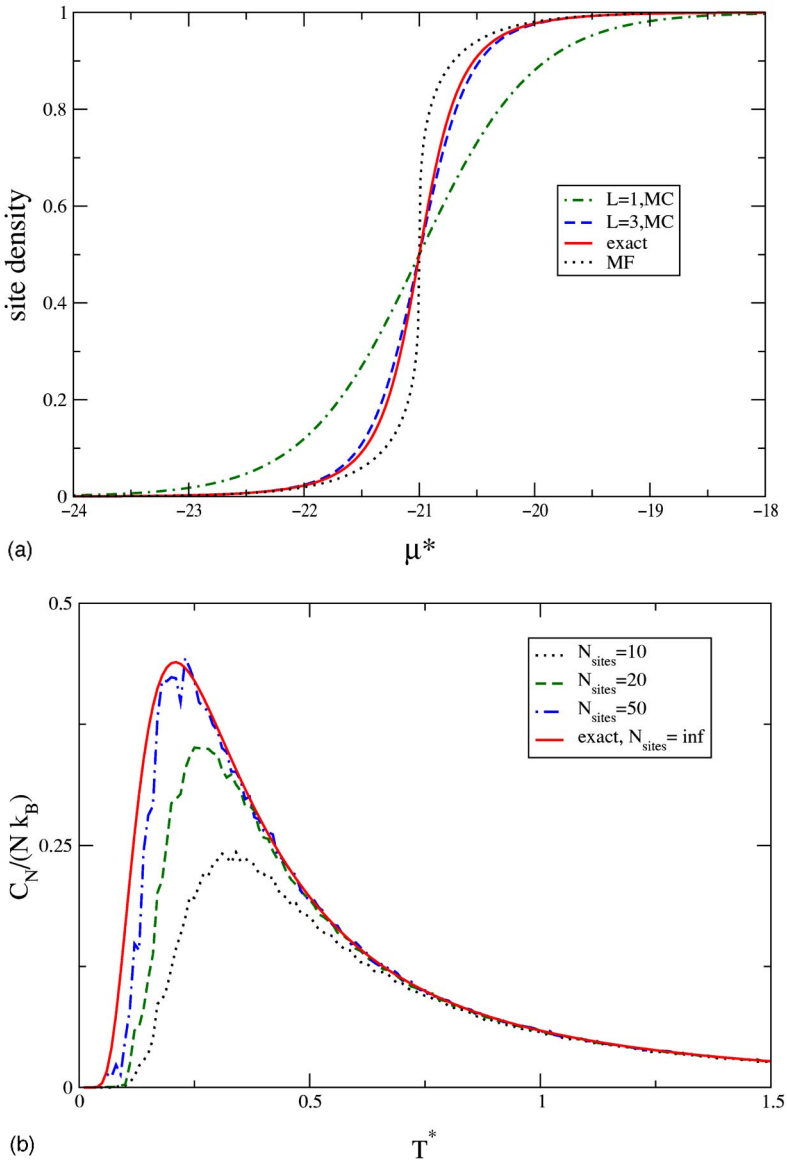

FIG. 2. Fractional site occupancy at $T^*=0.5$ for a purely 1D array of sites: (a) Occupancy as a function of reduced chemical potential. The exact analytic solution (full curve) is compared to GCMC simulations with various simulation cell sizes (1 and 3 sites), and to the MFT results (dotted curve). (b) Specific heat as a function of reduced temperature. Results of canonical MC simulations with various numbers of sites (at half-occupancy) are compared to the exact solution for an infinite system at half-occupancy.

II. MONTE CARLO METHOD

In the thermodynamic limit, a nanotube is a 1D system from the perspective of phase transition theory (only one length approaches infinity). Thus, it is expected that gases adsorbed in isolated nanotubes should behave thermodynamically like 1D systems. In Monte Carlo simulations, one represents the system with a unit cell of sites that is repeated periodically. In order to test the accuracy of the simulations for various periodic cell sizes, we first perform grand canonical Monte Carlo (GCMC) calculations for a purely 1D line of sites. Figure 2(a) shows a comparison between isotherms obtained with GCMC (for different cell sizes) from MFT, and the exact solution for an infinite Ising lattice gas [12]. Note first that a spurious singularity (an infinite slope) appears in the MFT curve, while no singularity is present in the exact and MC results. GCMC yields results very close to the exact results for cells consisting of 3 sites, replicated with periodic boundary conditions. We conclude that one does not need large cell sizes to simulate isotherms for such a 1D system. A similar conclusion was found by Swift *et al.* when modeling adsorption in a porous medium [6]. As seen in Fig. 2(b), specific heat results obtained from canonical Monte Carlo simulations are similar to the exact ones (at half-occupancy) for cells of about 50 sites (25 particles). The variation with number of sites in the cell is consistent with the thermodynamic relation

$$\int_0^\infty C_N(T)/NdT=[E(\infty)-E(0)]/N. \tag{2}$$

At half-occupancy, the energy per particle at $T=\infty$ is the same for any cell size; but at $T=0$, it depends on the number of particles present in one cell (N) because the ground state of the periodic system at half-occupancy consists of periodic islands of occupied sites: $E(0)=-\epsilon(N-1)$. Thus the heat capacity increases with N as seen in Fig. 2(b).

To make contact with our previous MF calculations for the system involving axial and shell sites, we take the unit

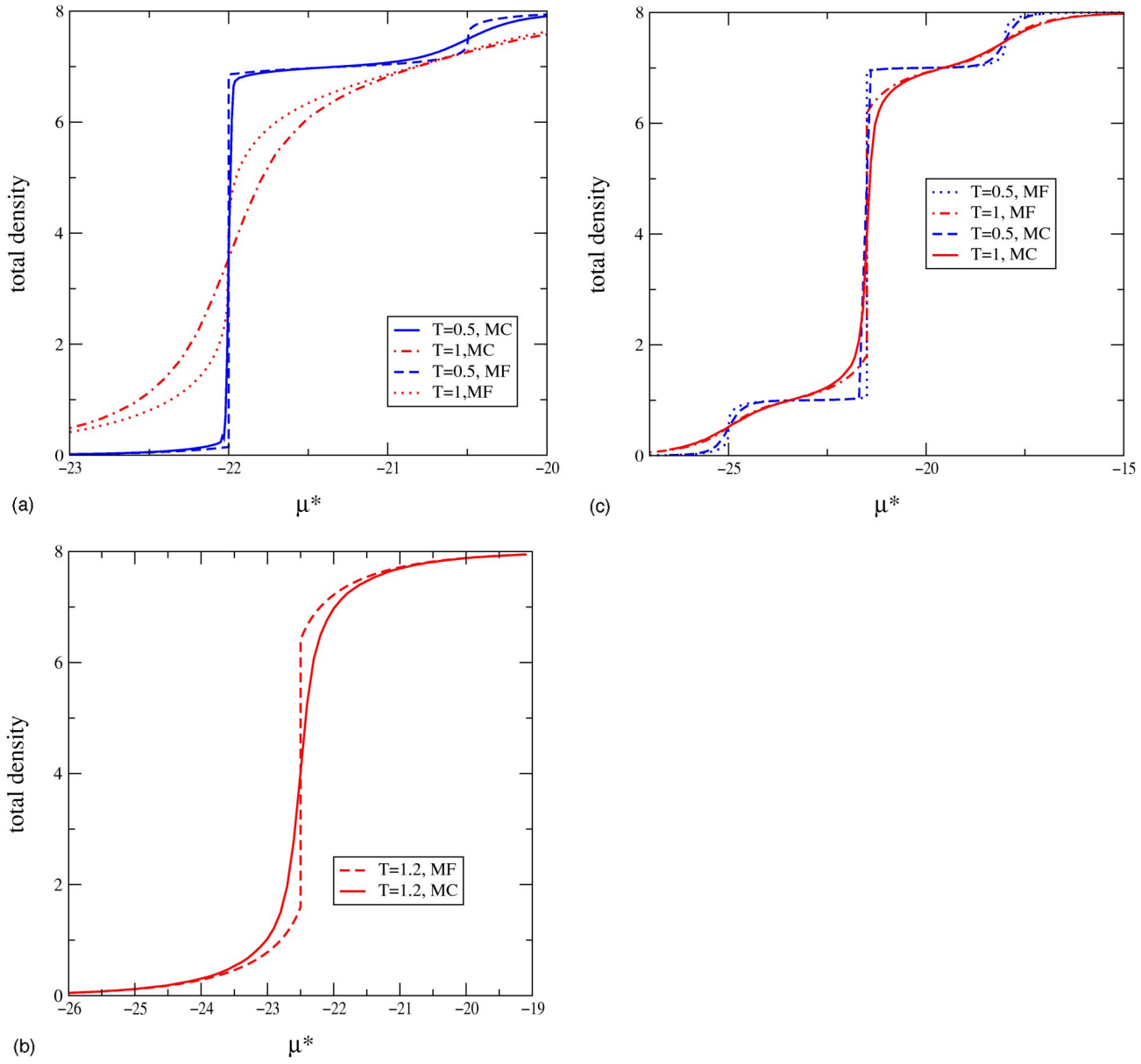

FIG. 3. Mean-field isotherms are compared to GCMC isotherms for three cases: (a) shell and axial energies differ appreciably ($V_s=20, V_a=12.5$) and axial-shell interaction is attractive ($\epsilon_{sa}<0$); (b) shell and axial energies are similar ($V_s=20, V_a=18$) and axial-shell interaction is attractive ($\epsilon_{sa}<0$); (c) shell and axial energies differ by an intermediate amount ($V_s=20, V_a=24$) and axial-shell interaction is repulsive ($\epsilon_{sa}>0$).

cell of the system to consist of one axial and seven shell sites. The cell replicated periodically in simulations is ten lattice constants long, meaning eighty sites in total. We perform simulations in the grand canonical ensemble to find the evolution of N with μ, and simulations in the canonical ensemble to find the specific heat $C_N(T)$ when the total (axial + shell) number of particles is fixed. The specific heat is obtained from energy fluctuations according to the formula:

$$C_N/(Nk_B)=(\langle E^2\rangle-\langle E\rangle^2)/(k_BT)^2. \tag{3}$$

Note that, in the canonical ensemble, even though N is fixed, the axial, and shell densities vary with T as particles migrate from one shell to the other. This transfer process makes an interesting contribution to the specific heat, as described in the following section.

III. RESULTS

Figures 3(a)–3(c) compare results from MFT and MC calculations of adsorption isotherms in three cases which differ in either the relation between V_a and V_s or the sign of the axial-shell interaction ϵ_{as}. The case illustrated in Fig. 3(a) is one for which the shell phase is energetically favored relative to the axial phase ($V_s<V_a$) and the axial-shell interaction is attractive ($\epsilon_{as}<0$). At $T^*=0.5$, the shell fills in a nearly

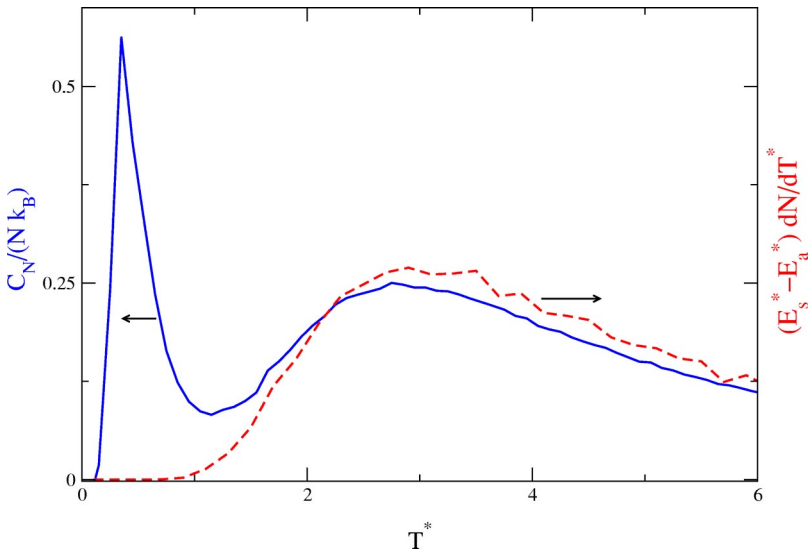

FIG. 4. Specific heat (full curve, left scale) and the transfer heat capacity (dashed curve, right scale) from shell to axial sites as a function of reduced temperature T^*, obtained with the parameter set (a) of Fig. 2.

discontinuous way in the MC calculation; this might be called a ''quasitransition'' because of that behavior. The MFT, in contrast, exhibits behavior characteristic of a first-order transition (discontinuity) at $T^*=0.5$. In fact, the MC solution is numerically quite close to that of the MFT, so that a transition might be (incorrectly) inferred from experimental data that looks like this. At the higher value, $T^*=1$, the MFT shows critical behavior (a divergent slope at half-occupancy of the shell sites) while the MC result shows a smoother shell-filling behavior. In Fig. 3(a), the MC results show the axial phase formation to be gradual at $T^*=0.5$, while the MFT behavior is that of a critical transition, since $T^*=z^*J/2=2^*\epsilon/4=0.5$ is the critical temperature of the axial phase transition (where z is the effective coordination number, 2 for this transition). Under these circumstances, the shell phase provides a spectator field, which affects the critical value of μ but not the critical temperature in the MFT.

Figure 3(b) displays rather different behavior of the isotherms, a consequence of the fact that V_a and V_s are very similar ($V_a=20$ and $V_s=18$). As a result, as discussed in I, there occurs a cooperative transition, in which both axial and shell sites fill together at the quasitransition. Moreover, because of the higher coordination number (including axial-shell attractions) in this case, the MFT critical temperature is pushed to a higher value than in the case (discussed above) of very different values of V_a and V_s. This feature of the MFT is shared with the quasitransition of the MC solution. Evidence for this statement is seen in the similar steepness of the isotherm at $T^*=1.2$ in Fig. 3(b) and that at $T^*=1.0$ in Fig. 3(a); both have $10-90\%$ widths $\Delta\mu^*\simeq 1$.

Figure 3(c) presents results that may seem counterintuitive at first sight. This behavior is a consequence of a repulsive axial-shell interaction, with $V_a<V_s$. In this case, the axial phase forms at a low value of μ^*, followed at higher μ^* by the appearance of the shell phase. The arrival of the shell phase, however, drives out the axial phase because of their mutual repulsion, so that the net increase in N is the difference between shell and axial occupancies ($6=7-1$). Eventually, at even higher μ, the axial phase finally returns to the pore. This behavior is precisely what is predicted in I with the MFT, as is seen in Fig. 2(c). This represents a situation where the two phases do not ''fit'' particularly comfort-

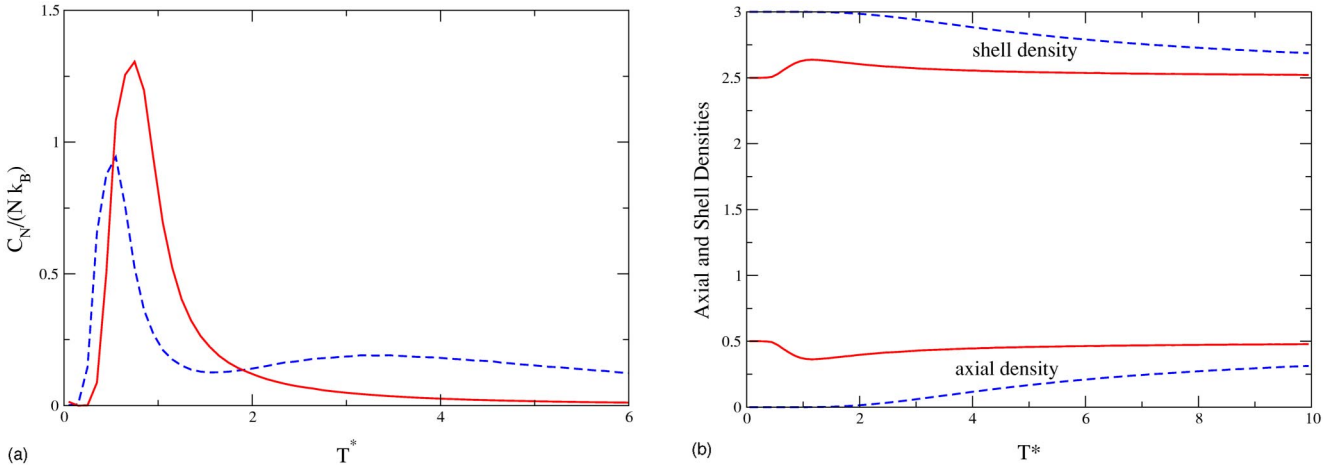

FIG. 5. ''Cooperative'' (full curve, $V_s=20, V_a=19$) vs ''normal'' (dashed curve, $V_s=20, V_a=10$) behavior in (a) specific heat calculations and (b) axial and shell densities.

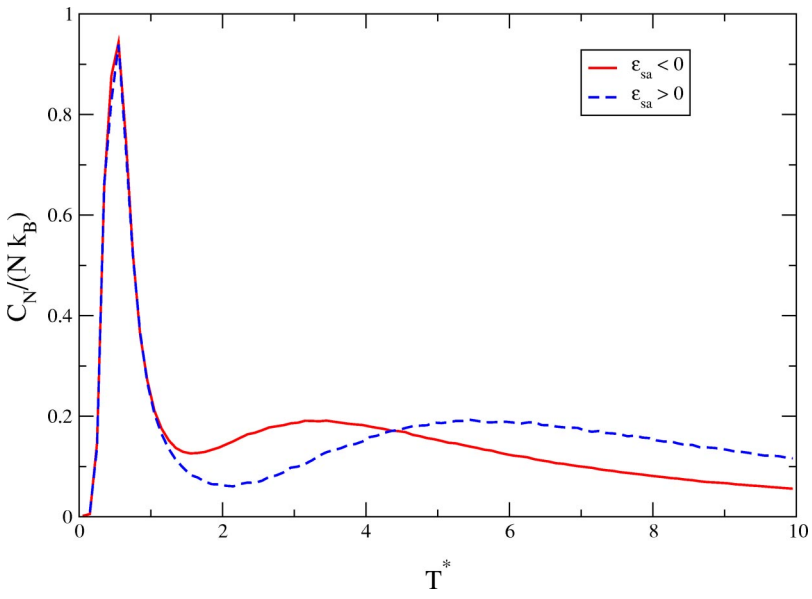

FIG. 6. Specific heat comparison between attractive ($\epsilon_{sa}<0$) and repulsive ($\epsilon_{sa}>0$) axial-shell interaction. The parameters used are: $V_s=20, V_a=10, N_p/N_s=1/2$ (where N_p and N_s are the number of particles and sites, respectively).

ably in the pore, but sufficient incentive, provided by μ, can induce their coexistence.

Figure 4 displays the specific heat $C_N(T)$ under the circumstances corresponding to Fig. 3(a), i.e., $V_s<V_a$ and an attractive axial-shell interaction. One observes two bumps in the data, near $T^*=0.3$ and $T^*=2.9$, respectively. At low T^*, all of the particles occupy shell sites (not filling them completely). The $T^*=0.3$ peak is associated with the loss of ordering among these particles; it would be a discontinuity in MFT (due to reaching the coexistence curve for the transition found in that model). The origin of the high T^* (broad peak) behavior can be appreciated from a comparison in Fig. 4 between $C_N(T)$ and $(E_s-E_a)dN_a/dT$. Here, the energy difference (E_s-E_a) equals the site energy difference V_s-V_a, plus a small correction due to the mutual interactions in the shell and axial phases. Quantitatively, the peak region is described by the expected relation based on this interpretation

$$C_N^{trans}(T^*)/(Nk_B)=(E_s^*-E_a^*)(dN_a/dT^*). \qquad (4)$$

The broad peaks in both curves have maxima near $T^*=3$. This similarity indicates that the peak is a kind of desorption peak, familiar in film adsorption data. The difference here is that ''desorption'' means a transfer of particles from the lower energy shell to the axial phase as T increases. This happens, as expected, when k_BT is of order the site's energy difference, V_s-V_a. The axial-shell transfer heat capacity peak is analogous also to the peak found in a recent study of adsorption on the outside of a bundle, attributed to the transfer of molecules from the groove to the quasi-2D surface of the tubes [11]. Similar behavior to that reported here has been found by Matranga *et al.* in simulations of CO2 within (10,10) nanotubes. As exemplified in Figs. 10 and 11 of their paper, increasing temperature causes excitation of the molecules from the shell phase to the tube's interior [13].

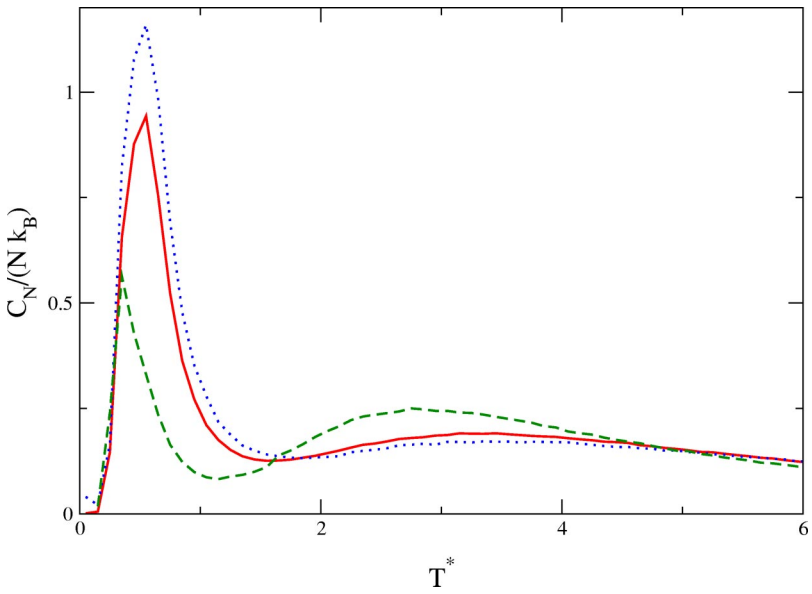

FIG. 7. Specific heat results for various number of particles: $N_p/N_s=1/2$ (full curve), $N_p/N_s=5/12$ (dotted curve), and $N_p/N_s=2/3$ (dashed curve). The parameters used are: $V_s=20, V_a=10$.

Figures 5(a) and 5(b) compare the behavior for two examples that differ in the size of the axial-shell energy difference $V_s - V_a$. One set of curves corresponds to the case of a large difference, just discussed, featuring the high T^* peak. The other set describes the cooperative quasitransition case, where the difference is small. The latter has its ordering peak at a higher T than the former, as discussed earlier; in addition, there is no particle transfer peak, as expected.

Figure 6 compares two situations differing in the sign of the axial-shell interaction. As expected, the transfer peak occurs at a lower T^* when this interaction is attractive than when it is repulsive; the reason is that the axial particles have a lower energy in the attractive case, so that the required excitation energy is smaller than in the repulsive case.

Finally, in Fig. 7 we explore the effects of varying shell occupancy fraction, at fixed interaction strength. A big difference between the curves appears in the low T^* peak. For shell filling fraction 2/3, the peak occurs near $T^* = 0.4$, lower than the other fillings' peak value, $T^* = 0.6$. This difference can be understood from the MFT predictions. In that case, the in-shell transfer term is due to evaporation from the condensed to the dilute phase. This process stops when the condensed phase is evaporated completely, i.e. when the system reaches the coexistence curve of the in-shell transition. The temperature at which that occurs is lower at 2/3 filling than near 1/2; the other curves shown are at 1/2 and 5/12, respectively. The other notable feature in Fig. 7 is that the transfer peak occurs at lower T^* in the 2/3 filling case. This is probably due to the fact that the axial phase particles have a lower energy in this case because of the attractive axial-shell interaction energy, which is larger in magnitude at high occupancy than at low occupancy.

IV. SUMMARY AND CONCLUSIONS

In this paper, we have presented results from MC simulations of a number of cases involving different energies and interactions. A common feature is that properties computed by MC simulations bear a close resemblance to those obtained from the MFT predictions. This finding might be surprising in view of the fact that the system is essentially one dimensional, meaning that the transitions in MFT are spurious. Nevertheless, as found previously in other systems [6], the MFT yields very reasonable predictions away from the transition points. This finding suggests the broad utility of the MFT, a convenient situation because of its simplicity. From the experimental point of view, the difference between the two approaches may not even be visible. One should not, therefore, be surprised to see MFT-like behavior in such experimental results.

In closing, we note an obvious limitation of the lattice-gas model-its inflexibility. Particles can occupy only a set of predetermined sites prescribed by the model. This means that a user of the model should think carefully about the choices of site and interaction energies. As indicated in I, a wide variety of behaviors can be found that depend on this set of parameters. Presumably, this reflects the variety seen in the many porous systems we are trying to describe.

ACKNOWLEDGMENT

This research was supported by NSF. We are grateful to Silvina Gatica for helpful comments.

[1] Lev D. Gelb, K.E. Gubbins, R. Radhakrishnan, and M. Sliwinska-Bartkowiak, Rep. Prog. Phys. **62**, 1573 (1999).
[2] L. Maibaum and D. Chandler, J. Chem. Phys. **107**, 1189 (2003).
[3] R.A. Trasca, M.M. Calbi, and M.W. Cole, Phys. Rev. E **65**, 061607 (2002).
[4] M. Takahashi, *Thermodynamics of 1D Solvable Models* (Cambridge University Press, Cambridge, U.K., 1999).
[5] M.E. Fisher, Phys. Rev. **162**, 480 (1967).
[6] M.R. Swift, E. Cheng, M.W. Cole, and J.R. Banavar, Phys. Rev. B **48**, 3124 (1993).
[7] R. Radhakrishnan and K.E. Gubbins, Phys. Rev. Lett. **79**, 2847 (1997).
[8] M.W. Cole, V.H. Crespi, G. Stan, C. Ebner, J.M. Hartman, S. Moroni, and M. Boninsegni, Phys. Rev. Lett. **84**, 3883 (2000).
[9] A.J. Ramirez-Pastor, T.P. Eggarter, V.D. Pereyra, and J.L. Riccardo, Phys. Rev. B **59**, 11 027 (1999).
[10] A.J. Ramirez-Pastor, J.L. Riccardo, and V.D. Pereyra, Surf. Sci. **411**, 294 (1998).
[11] M.M. Calbi and M.W. Cole, Phys. Rev. B **66**, 115413 (2002).
[12] R.K. Pathria, *Statistical Mechanics* (Butterworth-Heinemann, 1996), Chap. 12 (Eq. 16).
[13] C. Matranga, L. Chen, M. Smith, E. Bittner, J.K. Johnson, and B. Bockrath, J. Phys. Chem. B **107**, 12930 (2003).